An allometric scaling approach to estimate epiphytic bryophyte biomass in tropical montane cloud forests

Guan-Yu Lai[1], Hung-Chi Liu[1], Ariel J. Kuo[2], Cho-ying Huang[1,3,*]

[1]Department of Geography, National Taiwan University, Taipei 10617, Taiwan

[2]Department of Civil and Environmental Engineering, University of California, Los Angeles, CA 90024, USA

[3]Research Center for Future Earth, National Taiwan University, Taipei 10617, Taiwan

[*]Corresponding author

Tel: 886 2 33663733; E-mail: choying@ntu.edu.tw

Abstract

Epiphytic bryophytes (EB) are some of the most commonly found plant species in tropical montane cloud forests, and they play a disproportionate role in influencing the terrestrial hydrological and nutrient cycles. However, it is difficult to estimate the abundance of EB due to the nature of their "epiphytic" habitat. This study proposes an allometric scaling approach to measure EB biomass, implemented in 16,773 ha tropical montane cloud forests of northeastern Taiwan. A general allometry was developed to estimate EB biomass of 100 cm^2 circular-shaped mats (n = 131) and their central depths. A point-intercept instrument was invented to measure the depths of EB along tree trunks (n = 210) below 3-m from the ground level (sampled stem surface area [SSA]) in twenty-one 30 × 30 m plots. Biomass of EB of each point measure was derived using the general allometry and was aggregated across each SSA, and its performance was evaluated. Total EB biomass of a tree was estimated by referring to an *in-situ* conversion model and was interpolated for all trees in the plots (n = 1451). Finally, we assessed EB biomass density at the plot scale and preliminarily estimated EB biomass of the study region. The general EB biomass-depth allometry showed that the depth of an EB mat was a salient variable for biomass estimation ($R^2 = 0.72$, $p < 0.001$). The performance of upscaling from mats to SSA was satisfactory, which allowed us to further estimate mean (± standard deviation) EB biomass of the 21 plots (272 ± 104 kg ha^{-1}) and to provide preliminary estimation of the total EB biomass of 4562 Mg for the study region. Since a significant relationship between tree size and EB abundance is commonly found, regional EB biomass may be mapped by integrating our method and three-dimensional airborne data.

Keywords: conifer, diameter at breast height (DBH), lichen, liverwort, moss, scaling, Taiwan, tree size

1 INTRODUCTION

Bryophytes are rootless, non-vascular terrestrial plants such as mosses, liverworts and hornworts. Due to their primitive physiological characteristics, bryophytes are sensitive to the recent changes in climate such as increases in air temperatures (Aptroot & Van Herk 2007; Zotz & Bader 2009) and atmospheric carbon dioxide (Turetsky 2003), and decreases in precipitation (Gignac 2001). Epiphytic bryophytes (EB) are species that grow on the surface of a plant above the ground. They are some of the most representative lifeforms of tropical montane cloud forests (TMCF) (Barkman 1958; Smith 1982), which are ecosystems that experience frequent immersion of low altitude cloud (also known as "fog", exchangeably used hereafter) with high humidity. Tropical montane cloud forests, as suggested by their name, are mostly distributed over mountainous regions. While covering only about 0.14% (~30M ha) of the Earth's terrestrial surface (Bruijnzeel, Mulligan, & Scatena 2011) and 2.5% of tropical forests of the world (Bubb *et al.* 2004), they are the major water sources for lowland environments. As a result, TMCFs play a disproportionately-large role in the functioning of a global terrestrial ecosystem relative to their limited distribution.

Epiphytic bryophytes may obtain necessary water and nutrients for growth by intercepting parallel fog water (Stadtmüller 1987; Holwerda *et al.* 2010; Scholl, Eugster, & Burkard 2011). In some regions, EB are keystone species for providing water and essential nutrients to maintain the health of TMCFs (Gradstein 2008; Zotz & Bader 2009) and may affect carbon storage of an entire ecosystem. They may also influence the global hydrological cycle by modifying precipitation and evaporation levels (Rhoades 1995; Chang, Lai, & Wu 2002; Porada, Van Stan, & Kleidon 2018). In the recent decades, land use and land cover change (Ray *et al.* 2006), and the prevailing global trend of elevated temperatures (Still, Foster, & Schneider 1999; Foster

2001) may alter regional climate in tropics, resulting in substantial ramifications on EB (Benzing 1998) and eventually TMCF. As "canaries in the coal mine" (Gignac 2001), spatiotemporal dynamics of EB may be effective indicators for monitoring the regional and global climate changes. One of the very first steps in this research field is to quantify the abundance of EB, which has been a very challenging task due to nature of their habitats and diverse morphologies (McCune & Lesica 1992).

Biomass is a major metric to assess the abundance of plants (Bonham 2013). For EB, biomass is also a key indirect parameter to assess the capacity of TMCFs to intercept fog (Zotz & Vollrath 2003). The abundance of EB in TMCFs may be affected by microclimatic (e.g., humidity, temperature, luminosity) and host structural (such as tree size, height and density) attributes (Peck, Hong, & McCune 1995; Freiberg & Freiberg 2000; Nöske *et al.* 2008; Chen, Liu, & Wang 2010). Field survey approaches such as destructively sampling with interpolation on the ground for low stature (Ah-Peng *et al.* 2017) or fallen (Chen, Liu, & Wang 2010) trees, and using a ladder, rope (Hsu, Horng, & Kuo 2002; Nakanishi *et al.* 2016), high tower or crane (McCune *et al.* 1997; McCune *et al.* 2000) to reach tall trees have been commonly implemented to measure EB biomass (see Table 1 a comprehensive summary). However, field EB measurements have been known to be quite challenging to carry out, which made regional quantification impractical (Moffett & Lowman 1995; Barker & Pinard 2001). In this paper, we proposed a simple and effective field allometric scaling method to estimate EB biomass for TMCF, which combines small-scale destructive field biomass collection, vertical point intercept sampling conducted by a newly-invented instrument, and up-scaling the biomass estimation with a previously established *in-situ* equation and data interpolation.

2 MATERIALS AND METHODS

2.1 Study site

The study was focused on 16,773 ha TMCF of Chilan Mountain (24°98'N, 120°97'E) in northeastern Taiwan (the spatial boundary defined by referring to Schulz *et al.*, 2017). The precipitation in summer and winter consists of mostly orographic precipitation and tropical cyclones (regionally known as typhoons), and the northeastern monsoon, respectively. Annual precipitation and mean temperature of the site are 3,500 mm y^{-1} and 12.7°C, respectively. The mean (± standard deviation [SD]) elevation of the site is 1680 ± 343 m a.s.l., and mean slope (± SD) is 38.2° ± 13.4° ranging from 0° to 88.7°. The rugged terrain faces regular moist wind from the Pacific Ocean resulting in frequent occurrences of upslope fog approximately 300+ days of a year and 38% of the time (Lai *et al.* 2006). This humid bioclimate harbors a substantial amount of EB. There were 49 and 24 species observed in mature old-growth and regenerated forests, respectively, by a preliminary local inventory (Chang, Lai, & Wu 2002). The primary vegetation type of the TMCF is conifer forest, dominated by hinoki cypress (*Chamaecyparis obtusa* var. *formosana*) and Japanese cedar (*Cryptomeria japonica*). Bryophytes are the dominant epiphytic species of the region, occupying 93.5% of the total biomass (Deng 2006).

2.2 The patch scale EB biomass sampling and model development

The first step was to derive a general allometry for EB biomass, and six sites along the elevation gradient of 1200–1950 m a.s.l. were selected for sample collection (Figure S1). In the summer (May-October) of 2017, the center depth (e.g., from rhizoids to the top of a plant) of each EB species (n = 131; 113 liverworts, 17 mosses and 1 lichen) (for details of the species see the spreadsheet in Supplementary Information) within a randomly-selected 100 cm^2 circular patch of

100 a tree stem below 3 m above the ground was measured using a stainless steel ruler, and the
101 sample was removed using a gardening shovel. Only a single species in the patch with the
102 homogeneous depth was confirmed before the sample removal. The method has been applied
103 previously by Rodríguez-Quiel, Mendieta-Leiva and Bader (2019). We note that one lichen
104 sample was included in the model development due to the presence of a small portion of lichen
105 among EB. The samples were stored in sealed linear low-density polyethylene bags to maintain
106 moisture, then placed in an ice box and transported to a laboratory within eight hours after their
107 removal from host trees. The samples were cleaned of dead organic matter, suspended soil and
108 tree bark with tap water, dried in a 70°C biomass oven for at least 72 hours, and weighed using a
109 three decimal place electronic balance (LIBROR EB-430H, Shimadzu, Japan). In this study, EB
110 biomass was defined as the total sampled dry weight divided by the projected surface area of the
111 sample (mg cm^{-2}). The depth of EB was used as a unique trait for each independent sample to
112 develop EB biomass allometric equations:

113 $$W = \alpha D^{\beta} \quad (1)$$

114 where W is the EB biomass (mg cm^{-2}), D is the EB depth (cm), and α and β are the exponent
115 components for the model. A power model was selected to fit the data by referring to previous
116 studies (Niklas 1993; Niklas 2006) using R v. 3.5.0. (Stanford University; http://www.r-
117 project.org/). Consecutive values ranging from 0.01 to 2.0 with an interval of 0.01 were selected
118 for β with and without a fixed α value of 10 to derive an optimized model to fit the empirical
119 data using generalized least squares. The method (generalized least squares) was specifically
120 designed to minimize the effect of unequal variances, which were commonly observed in
121 ecological data (Pinheiro & Bates 2006). Three variance covariate functions, the exponential of a

variance covariate (varExp in R), power of a variance covariate (varPower) and constant plus power of a variance covariate (varConsPower), were used to modify regression of the fitted values and the residuals within the fitted model. The Akaike information criterion (AIC), the Bayesian information criterion (BIC) and log-likelihood were considered when facilitating model selection (Burnham & Anderson 2004). All statistical analyses were conducted using the "nlme" package in R (Pinheiro *et al.* 2019).

2.3 The tree scale EB biomass estimation

The main goal of this study was to implement a new field method for estimating EB biomass of TMCF at the regional scale. Once the allometric model (equation (1)) has been established, the next step was to estimate EB biomass of a tree, and we could then interpolate the estimate in the plot and regional scales. Twenty-one 30 × 30 m plots along the elevation gradient of 1260–1990 m a.s.l in Chilan Mountain of northeastern Taiwan were surveyed (Figure S1). Diameter at breast height (DBH) measured at 130 cm above the ground for each living tree with DBH ≥ 5 cm within 16 plots was recorded in July of 2016. The same approach was applied again to five more plots in January of 2019. During May-August of 2018 and January-February of 2019, we selected 10 trees (210 trees total) within each plot evenly distributed along the DBH gradient to interpolate EB biomass. Basal diameter (BD) of each sampled tree was also measured, and the relationship between basal area and DBH was investigated.

According to Johansson (1974) and Köhler *et al.* (2007), the majority of EB (in their case, 71–91%) were present at the lower part of a tree in TMCF, which may be utilized as a salient variable in estimating EB biomass of a tree. Therefore, a new field instrument was designed specifically for the estimation of EB biomass at the tree scale (Figure 1). From the ground to 300

cm of each sampled tree stem height, the EB depths (including the absence of EB with the depth of 0 cm) were recorded for every 30 cm vertical interval in several directions and were converted to biomass by referring to the allometry (equation (1)) and then averaged. The procedure was not vice versa due to the non-linearity of the allometry (a power model). We note that all trees in the plots were taller than 300 cm. The biomass of EB below 300 cm of a host tree was derived by taking the sampled stem surface area (SSA) into account. According to the visual inspection, the shape of the trunk from the ground to 130 cm was defined as a truncated cone and from 130 cm to 300 cm from the ground as a cylinder. Accordingly, the surface area (cm^2) of the trunk below 3 m (SSA) was calculated by referring to equations (2) and (3):

$$SSA = 170 \times \pi \times DBH + \pi \times l \times \left(\frac{BD}{2} + \frac{DBH}{2}\right) \quad (2)$$

$$l = \sqrt{130^2 + (\frac{BD}{2} - \frac{DBH}{2})^2} \quad (3)$$

where SSA (cm^2), l (cm), DBH (cm) and BD (cm) are sampled stem area, slant length of the cone, diameter at breast height and basal diameter, respectively. The sampled trees with DBH larger than 20 cm were recorded in eight directions (north, northeast, east, southeast, south, southwest, west and northwest) otherwise in just four major cardinal directions by referring to a compass. In August 2019, we stripped EB mats of SSA from 30 randomly selected and widely-distributed trees of different sizes to verify the estimation.

2.4 EB biomass up-scaling

The biomass of EB of 10 sampled tree was estimated by referring to equation (4):

$$ln(M_{Total}) = 0.99ln(DBH) + 0.68ln(M_{SSA}) - 1.195 \quad (4)$$

where M_{total} and M_{SSA} are EB biomass (kg) of total surface area and SSA of a tree, respectively, according to the *in-situ* destructive measurement by stripping EB from 10 harvested hinoki trees ($R^2 = 0.99$, $p < 0.001$) (Deng 2006). Since the intercept of equation (4) is negative, resulting in negative values for small trees, a fixed ratio of 1.3 was then applied according to Deng (2006) for those trees. Sampled stem area of all trees (SSA_{total}) in a plot was then estimated with the knowledge of DBH and DBH-BD of each tree (equations (2) and (3)), and EB biomass (M_{total}, kg) (equation 5) and its density (kg ha^{-1}) of a plot may be estimated by referring to equation (5) with the knowledge of EB biomass ($M_{sampled}$) on SSA ($SSA_{sampled}$) of 10 sampled trees.

$$\frac{SSA_{total}}{SSA_{sa}} = \frac{M_{total}}{M_{sampled}} \quad (5)$$

Literature search was conducted in Google Scholar (https://scholar.google.com/) with the keywords “epiphytic bryophyte” and “biomass” for a general comparison of EB biomass density (with basic bioclimatic information). We note that for the sake of quality control, non-refereed articles such as graduate theses and conference proceedings were excluded. Finally, since the stand characteristics of selected plots were quite representative of the region by referring to Wang and Huang (2012), Hu and Huang (2019) and several local inventory data, EB biomass of TMCF in Chilan Mountain may be estimated after taking the areal size of the region (16,773 ha) into account.

3 RESULTS

3.1 Epiphytic bryophytes biomass allometry

In this study, we collected 100 cm^2 circular-shaped EB samples (n = 131) from six forest stands in Chilan Mountain along an elevation gradient. The mean (± SD [minimum–maximum])

sampled EB depth and biomass were 4.5 ± 2.9 cm (0.3–13.7 cm) and 36.0 ± 20.3 (6.2–99.3) mg cm^{-2}, respectively. Significant positive correlations ($p < 0.005$) were found among EB depth and biomass with different regression models (Table 2). Performance of the allometric equation of the power of variance covariate function ($R^2 = 0.72$, $p < 0.0001$) with smaller AIC and BIC and greater log likelihood was superior to other models, and the model was selected for further analyses (Figure 2).

3.2 The tree-scale EB biomass estimation

Ten trees evenly distributed along the DBH gradient of each plot (total 210 trees) were selected to investigate the relationship between DBH and BD of EB-hosted trees. The mean (± SD [minimum–maximum]) DBH and BD of sampled trees were 33.5 ± 27.8 (7.6–128.7) cm and 49.5 ± 34.5 (9.9–186.2) cm, respectively. High correlation ($R^2 = 0.94$, $p < 0.0001$) was found between DBH and BD (Figure S2). With this information, we computed SSA in the plots by referring to equations (2) and (3). The statistics (mean ± SD [minimum–maximum]) of SSA was 3.5 ± 2.8 (0.81–13.5) m^2. Mean (± SD [minimum–maximum]) EB depth of the 210 sampled trees was 1.1 ± 0.6 (0.1–3.1) cm, and the data was injected into the allometry (Figure 2) to yield EB biomass (mean ± SD [minimum–maximum]) of 10.2 ± 5.2 (0.7–26.1) mg cm^{-2} (or 402.2 ± 478.9 [8.3–2856.6] g) on SSA. We note that there was a significant positive curvilinear relationship ($p < 0.001$) between DBH of the sampled tree and EB biomass on SSA (Figure 3).

Biomass of epiphytic bryophytes on 30 randomly selected trees with mean (± SD, minimum–maximum) DBH of 26.2 ± 21.5 (5.7–93.0) cm was destructively collected to verify the proposed approach of upscaling the patch scale estimation (Figure 2) to SSA. Overall, the performance was satisfactory (Figure 4) and all samples but one outlier ($R^2 = 0.82$ and 0.95

without the outlier, $p < 0.0001$ for both model) were close to the 1:1 line (slope = 0.93 and 0.95 without the outlier, $p > 0.8$ for the intercepts of both models) with the mean absolute difference of 77.3 g (35.2% of the mean estimate) or 56.3 g (25.2% of the mean estimate) without the outlier. The outlier may be possibly due to rotten and soften tree barks underneath the EB mats (observed during the sample cleaning), and the depth of tree bark may have been included in the EB depth measurement, resulting in pronounced over-estimation. By applying the *in-situ* conversion function (equation (4)), the EB biomass (mean ± SD [minimum–maximum]) for each sampled tree within the plots was estimated (818.3 ± 1335.1 [12.9–7279.1]) g (n = 210).

3.3 The plot and regional scales EB biomass estimation

Mean (± SD [minimum–maximum]) DBH of the trees (n = 1451) within twenty-one plots was 20.3 ± 17.5 cm (5.0–176.0 cm) (detailed plot-scale statistics of forest stands see Table S1). The EB biomass (and biomass density) for each plot can be interpolated by referring to the EB biomass of 10 sampled trees within each plot with the mean ± SD (minimum–maximum) of 24.5 ± 9.4 (8.8-39.0) kg (or 272.0 ± 104.0 [97.9–433.3] kg ha^{-1}). Twenty-one refereed papers were found, and 86% (18/21) of the studies reported higher EB biomass density values than our mean plot/stand scale estimation (Table 1). Finally, with the knowledge of the plot-scale mean EB biomass density, we provided the preliminary estimation of the total EB biomass of 4562 Mg for the 16,773 ha TMCF of Chilan Mountain.

4 DISCUSSION

Epiphytic bryophytes are some of the most quintessential species characterizing mid-altitude tropical montane cloud forests (Bruijnzeel, Scatena, & Hamilton 2011) and play a pivotal role in influencing the global hydrological cycle (Porada, Van Stan, & Kleidon 2018). Due to the

diverse morphology of the species and their "epiphytic" habitat, it is difficult to quantify the abundance of EB. In this study, we propose a novel field protocol for regional EB biomass estimation. Our discussion will mainly focus on (1) EB depth-biomass allometry, (2) scaling of EB biomass from the patch to the regional scale, and (3) limitation and future directions.

4.1 The patch scale EB depth-biomass allometry

In this study, *in-situ* general allometric equations were developed to estimate the biomass of a 100 cm^2 circular patch of EB using the central depth of the sample (Figure 2). The performance was satisfactory, even though the morphology of EB is much more diverse than most vascular plants. Plant allometry focuses on relationships between plant body size and biomass, production, population density or other abundance related dependent variables (Enquist, Brown, & West 1998; Enquist *et al.* 1999). Stanton and Reeb (2016) suggested that some characteristics of bryophytes may be allometrically scaled like vascular plants, which was verified in this study. The mean exponent of the five selected power models was 0.75 (3/4) (Table 2), which agrees with the 3/4 power law (Kleiber 1947) and is similar to the constant scaling exponents over a wide range of vascular plant size, often with quarter-powers in metabolic scaling theory using biomass as an independent variable (West, Brown, & Enquist 1997; West, Brown, & Enquist 1999). However, epiphytic bryophytes are non-vascular plants composed of a simple stem, which has a limited role in transporting moisture and nutrients through conducting tissues and does not follow the vascular transport system as a self-similar, fractal-like branching network (Ligrone, Duckett, & Renzaglia 2000). Two major branching forms of bryophytes are sympodial with connected modules of equal level and monopodial (Stanton & Reeb 2016). For most vascular plants, the branching bifurcation is two (Enquist *et al.* 2007), and the height is 1/4 exponent of mass (West, Brown, & Enquist 1999). It was different to our empirical observation,

252 although the sampling unit was a mat but not an individual. This could verify that the basic
253 assumption of an organism's self-similar branching network plays a major role in governing the
254 allometric relationship.

255 **4.2 Up-scaling of EB biomass**

256 A point-intercept field instrument was invented in this study to facilitate sampling EB height data
257 along a tree stem, which were then used as an independent variable to estimate EB biomass
258 (Figure 2) and EB biomass of SSA, and later extrapolate to the tree scale using an *in-situ*
259 conversion equation (Equation (4)). The distribution of EB biomass on a tree could be very
260 sensitive to the ambient environment (McCune 1993; Sillett & Antoine 2004). Therefore, we
261 measured the depth of EB in four and eight directions for small (DBH ≤ 20 cm) and large (DBH
262 > 20 cm) trees, respectively, which may reduce microclimate-induced biases. The method was
263 efficient, taking about 15 minutes for the four-direction measurement and double that amount of
264 time for the eight-direction measurement. This may permit rapid sampling to obtain a large
265 sample size (Table 1). With proper sampling design and data inter/extrapolation, we may be able
266 to estimate EB biomass in a large region. Mean biomass density of EB estimated in this study
267 was similar to the one conducted in the same region (230 kg ha^{-1}) but within a much smaller
268 spatial extent using a destructive tree harvesting approach (Deng 2006). Our mean plot (forest
269 stand) scale estimation of EB biomass density falls within the lower half of the EB biomass
270 density global synthesis data (Table 1). It is challenging to make a fair comparison since those
271 previous studies were conducted using different data collection methods over a wide range of
272 spatial extents. However, in terms of efficiency, the proposed new approach is indeed superior to
273 other sampling methods implementing for the sampling of 210 EB host trees in this study.

This point-intercept approach should also be applicable for the estimation of ground bryophyte biomass, and facilitates the estimation of overall abundance of bryophytes in an ecosystem. This is a pivotal but rarely available parameter, and has a major impact on regulating the terrestrial hydrological cycles (Porada, Van Stan, & Kleidon 2018). This study focused on the height of a tree below 3 m from the ground, where the majority of EB are present (Trynoski & Glime 1982) (Figure 1B). The sampled stem area may be further extended with aids of a foldable ladder.

4.3 Limitation and future directions

One potential research limit is that the tree scale EB biomass estimation, which was extrapolated from the estimation on SSA (equation 4), could not be validated with empirical data. The task is rather difficult and may be impractical for the study region. It requires tree climbing or destructive tree harvesting to strip EB of an entire tree. However, the support of tree climbing was not available during the time of conducting this study, and it could be risky to climb a small-size tree without reliable support for a climber's body weight. Logging for both natural and plantation forests has been completely forbidden in Taiwan since 1991. Therefore, the latter option may not be possible due to the local regulation. In the future, we might be able to take the advantage of tropical cyclone-induced fallen logs and harvest EB biomass at the ground level, since the island is located in a typhoon-prone region (Chi *et al.* 2015). However, this sampling approach could be biased since the probability of the strong wind induced tree falling may be associated with topography (Mitchell 2013), which also plays a pivotal role in governing the abundance of EB (Werner *et al.* 2012).

It is extremely challenging to non-destructively measure EB biomass, and a new field

296 approach was developed in this study to tackle this task. This is crucial because the age of EB on
297 a tree could be almost as old as the age of the host tree (Kimmerer 2003), and it may require
298 many years of recovery after the removal of samples (Fenton, Frego, & Sims 2003). It may be
299 useful to further generalize the EB allometry (see the supplementary spreadsheet data) to make it
300 applicable for other settings. According to this study (Figure 3) and some previous literature
301 (Hsu, Horng, & Kuo 2002; Köhler *et al.* 2007; Chen, Liu, & Wang 2010), we found that there
302 may be a significant relationship between the tree size and the abundance of EB. With the
303 availability of a three-dimensional tree size spatial layer at the regional scale derived from high
304 spatial resolution airborne lidar (light detection and ranging) or aerial photographic point cloud
305 data (Chung *et al.* 2019; Kellner *et al.* 2019), we may be able to map EB biomass over a vast
306 region.

307 **ACKNOWLEDGEMENTS**

308 We appreciate Jun Zhang and Hong-You Lin for providing field assistance. This study was
309 sponsored by the Ministry of Science and Technology of Taiwan (MOST 106-2633-M-002-
310 002-), National Taiwan University EcoNTU project (106R104516), and the NTU Research
311 Center for Future Earth from the Featured Areas Research Center Program within the
312 framework of the Higher Education Sprout Project by the Ministry of Education in Taiwan.

313 **AUTHORS' CONTRIBUTIONS**

314 GYL and CyH conceived the idea and developed the method for this research and led the
315 writing of the manuscript; GYL, AJK and HCL analyzed the data. All authors collected field
316 data and contributed critically to the drafts and gave final approval for publication.

317 **DATA AVAILABILITY**

318 Data used to derive epiphytic bryophyte allometry can be found in Supplementary Information.

REFERENCES

Ah-Peng, C., Cardoso, A. W., Flores, O., West, A., Wilding, N., Strasberg, D., & Hedderson, T. A. (2017). The role of epiphytic bryophytes in interception, storage, and the regulated release of atmospheric moisture in a tropical montane cloud forest. *Journal of Hydrology, 548*, 665–673. https://doi.org/10.1016/j.jhydrol.2017.03.043

Aptroot, A., & Van Herk, C. (2007). Further evidence of the effects of global warming on lichens, particularly those with Trentepohlia phycobionts. *Environmental Pollution, 146*, 293–298. https://doi.org/10.1016/j.envpol.2006.03.018

Barker, M. G., & Pinard, M. A. (2001). Forest canopy research: sampling problems, and some solutions. In K. E. Linsenmair, A. J. Davis, B. Fiala, & M. R. Speight (Eds), *Tropical forest canopies: ecology and management, Forestry Sciences, vol 69* (pp. 23–38). Dordrecht, Netherlands: Springer. https://doi.org/10.1023/A:1017584130692

Barkman, J. J. (1958). *Phytosociology and ecology of cryptogamic epiphytes: including a taxonomic survey and description of their vegetation units in Europe*. Assen, Netherlands: Van Gorcum.

Benzing, D. H. (1998). Vulnerabilities of tropical forests to climate change: the significance of resident epiphytes. *Climatic Change, 39*, 519–540. https://doi.org/10.1023/a:1005312307709

Bonham, C. D. (2013). *Measurements for Terrestrial Vegetation*. West Sussex, UK: John Wiley & Sons. https://doi.org/10.1002/9781118534540

Bruijnzeel, L., Mulligan, M., & Scatena, F. N. (2011). Hydrometeorology of tropical montane cloud forests: emerging patterns. *Hydrological Processes, 25*, 465–498. https://doi.org/10.1002/hyp.7974

Bruijnzeel, L. A., Scatena, F. N., & Hamilton, L. S. (2011). *Tropical Montane Cloud Forests: Science for Conservation and Management (International Hydrology Series)*. Cambridge, UK: Cambridge University Press. https://doi.org/10.1017/CBO9780511778384

Bubb, P., May, I. A., Miles, L., & Sayer, J. (2004). *Cloud Forest Agenda*. Cambridge, UK: UNEP-World Conservation Monitoring Centre.

Burnham, K. P., & Anderson, D. R. (2004). Multimodel inference: understanding AIC and BIC in model selection. *Sociological Methods & Research, 33*, 261–304. https://doi.org/10.1177/0049124104268644

Chang, S.-C., Lai, I.-L., & Wu, J.-T. (2002). Estimation of fog deposition on epiphytic bryophytes in a subtropical montane forest ecosystem in northeastern Taiwan. *Atmospheric Research, 64*, 159–167. https://doi.org/10.1016/S0169-8095(02)00088-1

Chantanaorrapint, S., & Frahm, J.-P. (2011). Biomass and selected ecological factors of epiphytic bryophyte along altitudinal gradients in Southern Thailand. *Songklanakarin Journal of Science & Technology, 33,* 625–632.

Chen, L., Liu, W. y., & Wang, G. s. (2010). Estimation of epiphytic biomass and nutrient pools in the subtropical montane cloud forest in the Ailao Mountains, south-western China. *Ecological Research, 25*, 315–325. https://doi.org/10.1007/s11284-009-0659-5

Chi, C.-H., McEwan, R. W., Chang, C.-T., Zheng, C., Yang, Z., Chiang, J.-M., & Lin, T.-C. (2015). Typhoon disturbance mediates elevational patterns of forest structure, but not species diversity, in humid monsoon Asia. *Ecosystems, 18*, 1410–1423.

Chung, C.-H., Wang, C.-H., Hsieh, H.-C., & Huang, C.-Y. (2019). Comparison of forest canopy height profiles in a mountainous region of Taiwan derived from airborne lidar and

364 unmanned aerial vehicle imagery. *GIScience & Remote Sensing*, *56*, 1289–1304.
365 https://doi.org/10.1080/15481603.2019.1627044
366 Coxson, D. S. (1991). Nutrient release from epiphytic bryophytes in tropical montane rain forest
367 (Guadeloupe). *Canadian Journal of Botany, 69*, 2122–2129. https://doi.org/10.1139/b91-
368 266
369 Deng, Z.-H. (2006). The composition, distribution, and biomass of epiphytic bryophytes of a
370 naturally regenerated Chamaecyparis obtusa var. formosana forest. *Master Thesis*,
371 Department of Natural Resources and Environment Studies, College of Environment
372 Studies, National Donghua University, Hualien, Taiwan.
373 Edwards, P., & Grubb, P. (1977). Studies of mineral cycling in a montane rain forest in New
374 Guinea: I. The distribution of organic matter in the vegetation and soil. *Journal of*
375 *Ecology*, *65*, 943–969. https://doi.org/10.2307/2259387
376 Enquist, B. J., Brown, J. H., & West, G. B. (1998). Allometric scaling of plant energetics and
377 population density. *Nature, 395*, 163–165. https://doi.org/10.1038/25977
378 Enquist, B. J., Kerkhoff, A. J., Huxman, T. E., & Economo, E. P. (2007). Adaptive differences in
379 plant physiology and ecosystem paradoxes: insights from metabolic scaling theory.
380 *Global Change Biology, 13*, 591–609. https://doi.org/10.1111/j.1365-2486.2006.01222.x
381 Enquist, B. J., West, G. B., Charnov, E. L., & Brown, J. H. (1999). Allometric scaling of
382 production and life-history variation in vascular plants. *Nature, 401*, 907–911.
383 https://doi.org/10.1038/44819
384 Fenton, N. J., Frego, K. A., & Sims, M. R. (2003). Changes in forest floor bryophyte (moss and
385 liverwort) communities 4 years after forest harvest. *Canadian Journal of Botany, 81*,
386 714–731. https://doi.org/10.1139/b03-063
387 Foster, P. (2001). The potential negative impacts of global climate change on tropical montane
388 cloud forests. *Earth-Science Reviews, 55*, 73–106. https://doi.org/10.1016/S0012-
389 8252(01)00056-3
390 Freiberg, M., & Freiberg, E. (2000). Epiphyte diversity and biomass in the canopy of lowland
391 and montane forests in Ecuador. *Journal of Tropical Ecology, 16*, 673–688.
392 https://doi.org/10.1017/S0266467400001644
393 Gehrig-Downie, C., Obregón, A., Bendix, J., & Gradstein, S. R. (2011). Epiphyte biomass and
394 canopy microclimate in the tropical lowland cloud forest of French Guiana. *Biotropica,*
395 *43*, 591–596. https://doi.org/10.1111/j.1744-7429.2010.00745.x
396 Gignac, L. D. (2001). Bryophytes as indicators of climate change. *The Bryologist, 104*, 410–420.
397 Gradstein, S. R. (2008). Epiphytes of tropical montane forests—impact of deforestation and
398 climate change. *Göttingen Centre for Biodiversity and Ecology. Biodiversity and Ecology*
399 *Series, 2*, 51–65.
400 Häger, A., & Dohrenbusch, A. (2011). Hydrometeorology and structure of tropical montane
401 cloud forests under contrasting biophysical conditions in north-western Costa Rica.
402 *Hydrological Processes, 25*, 392–401. https://doi.org/10.1002/hyp.7726
403 Hölscher, D., Köhler, L., van Dijk, A. I., & Bruijnzeel, L. S. (2004). The importance of epiphytes
404 to total rainfall interception by a tropical montane rain forest in Costa Rica. *Journal of*
405 *Hydrology, 292*, 308–322. https://doi.org/10.1016/j.jhydrol.2004.01.015
406 Hofstede, R. G., Wolf, J. H., & Benzing, D. H. (1993). Epiphytic biomass and nutrient status of a
407 Colombian upper montane rain forest. *Selbyana*, *14*, 37–45.
408 Holwerda, F., Bruijnzeel, L., Muñoz-Villers, L., Equihua, M., & Asbjornsen, H. (2010). Rainfall
409 and cloud water interception in mature and secondary lower montane cloud forests of

central Veracruz, Mexico. *Journal of Hydrology, 384*, 84–96. https://doi.org/10.1016/j.jhydrol.2010.01.012

Hsu, C.-C., Horng, F.-W., & Kuo, C.-M. (2002). Epiphyte biomass and nutrient capital of a moist subtropical forest in north-eastern Taiwan. *Journal of Tropical Ecology, 18*, 659–670. https://doi.org/10.1017/S0266467402002432

Hu, K.-T., & Huang, C.-y. (2019). A metabolic scaling theory-driven remote sensing approach to map spatiotemporal dynamics of litterfall in a tropical montane cloud forest. *International Journal of Applied Earth Observation and Geoinformation, 82*, 101896. https://doi.org/10.1016/j.jag.2019.06.006

Johansson, D. (1974). Ecology of vascular epiphytes in West African rain forest. *Acta Phytogeographica Seucica, 59*, 1–136.

Köhler, L., Tobón, C., Frumau, K. A., & Bruijnzeel, L. S. (2007). Biomass and water storage dynamics of epiphytes in old-growth and secondary montane cloud forest stands in Costa Rica. *Plant Ecology, 193*, 171–184. https://doi.org/10.1007/s11258-006-9256-7

Kürschner, H., & Parolly, G. (2004). Phytomass and water-storing capacity of epiphytic rain forest bryophyte communities in S Ecuador. *Botanische Jahrbücher, 125*, 489–504. https://doi.org/10.1127/0006-8152/2004/0125-0489

Kellner, J. R., Albert, L. P., Burley, J. T., & Cushman, K. (2019). The case for remote sensing of individual plants. *American Journal of Botany, 106*, 1139–1142. https://doi.org/10.1002/ajb2.1347

Kimmerer, R. W. (2003). *Gathering Moss: A Natural and Cultural History of Mosses*. Oregon, US: Oregon State University Press.

Kleiber, M. (1947). Body size and metabolic rate. *Physiological Reviews, 27*, 511–541. https://doi.org/10.1152/physrev.1947.27.4.511

Lai, I., Chang, S.-C., Lin, P.-H., Chou, C.-H., & Wu, J.-T. (2006). Climatic characteristics of the subtropical mountainous cloud forest at the Yuanyang Lake long-term ecological research site, Taiwan. *Taiwania, 51*, 317–329. https://doi.org/10.6165/tai.2006.51(4).317

Ligrone, R., Duckett, J., & Renzaglia, K. (2000). Conducting tissues and phyletic relationships of bryophytes. *Philosophical Transactions of the Royal Society of London. Series B: Biological Sciences, 355*, 795–813. https://doi.org/10.1098/rstb.2000.0616

McCune, B. (1993). Gradients in epiphyte biomass in three Pseudotsuga-Tsuga forests of different ages in western Oregon and Washington. *The Bryologist, 96*, 405–411. https://doi.org/10.2307/3243870

McCune, B., Amsberry, K., Camacho, F., Clery, S., Cole, C., Emerson, C., Felder, G., French, P., Greene, D., & Harris, R. (1997). Vertical profile of epiphytes in a Pacific Northwest old-growth forest. *Northwest Science, 71*, 145–152.

McCune, B., & Lesica, P. (1992). The trade-off between species capture and quantitative accuracy in ecological inventory of lichens and bryophytes in forests in Montana. *The Bryologist*, *95*, 296–304. https://doi.org/10.2307/3243488

McCune, B., Rosentreter, R., Ponzetti, J. M., & Shaw, D. C. (2000). Epiphyte habitats in an old conifer forest in western Washington, USA. *The Bryologist, 103*, 417–428. https://doi.org/10.1639/0007-2745(2000)103[0417:EHIAOC]2.0.CO;2

Mitchell, S. (2013). Wind as a natural disturbance agent in forests: a synthesis. *Forestry: An International Journal of Forest Research, 86*, 147–157. https://doi.org/10.1093/forestry/cps058

Moffett, M. W., & Lowman, M. D. (1995). Canopy Access Techniques. In M. W. Moffett, & M.

456 D. Lowman (Eds), *Forest canopies* (pp. 3–26). San Diego: Academic Press.
457 Nöske, N. M., Hilt, N., Werner, F. A., Brehm, G., Fiedler, K., Sipman, H. J., & Gradstein, S. R.
458 (2008). Disturbance effects on diversity of epiphytes and moths in a montane forest in
459 Ecuador. *Basic and Applied Ecology, 9*, 4–12. https://doi.org/10.1016/j.baae.2007.06.014
460 Nadkarni, N. M. (1984a). Biomass and mineral capital of epiphytes in an Acer macrophyllum
461 community of a temperate moist coniferous forest, Olympic Peninsula, Washington State.
462 *Canadian Journal of Botany, 62*, 2223–2228. https://doi.org/10.1139/b84-302
463 Nadkarni, N. M. (1984b). Epiphyte biomass and nutrient capital of a neotropical elfin forest.
464 *Biotropica*, 249–256. https://doi.org/10.2307/2387932
465 Nadkarni, N. M., Schaefer, D., Matelson, T. J., & Solano, R. (2004). Biomass and nutrient pools
466 of canopy and terrestrial components in a primary and a secondary montane cloud forest,
467 Costa Rica. *Forest Ecology and Management, 198*, 223–236.
468 https://doi.org/10.1016/j.foreco.2004.04.011
469 Nakanishi, A., Sungpalee, W., Sri-Ngernyuang, K., & Kanzaki, M. (2016). Large variations in
470 composition and spatial distribution of epiphyte biomass on large trees in a tropical
471 montane forest of northern Thailand. *Plant Ecology, 217*, 1157–1169.
472 https://doi.org/10.1007/s11258-016-0640-7
473 Niklas, K. J. (1993). The allometry of plant reproductive biomass and stem diameter. *American*
474 *Journal of Botany, 80*, 461–467. https://doi.org/10.2307/2445392
475 Niklas, K. J. (2006). A phyletic perspective on the allometry of plant biomass-partitioning
476 patterns and functionally equivalent organ-categories. *New Phytologist, 171*, 27–40.
477 https://doi.org/10.1111/j.1469-8137.2006.01760.x
478 Peck, J. E., Hong, W. S., & McCune, B. (1995). Diversity of epiphytic bryophytes on three host
479 tree species, thermal Meadow, Hotsprings Island, Queen Charlotte Islands, Canada. The
480 *Bryologist*, *98*, 123–128. https://doi.org/10.2307/3243648
481 Pentecost, A. (1998). Some observations on the biomass and distribution of cryptogamic
482 epiphytes in the upper montane forest of the Rwenzori Mountains, Uganda. *Global*
483 *Ecology & Biogeography Letters, 7*, 273–284. https://doi.org/10.2307/2997601
484 Pinheiro, J., & Bates, D. (2006). Mixed-effects models in S and S-PLUS. New York: Springer
485 Science & Business Media. https://doi.org/10.1007/b98882
486 Pinheiro, J., Bates, D., DebRoy, S., Sarkar, D., & Team, R. C. (2019). nlme: Linear and nonlinear
487 mixed effects models. *R Package Version 3.1-141,* 3**,** 111. Retrieved from https://cran.r-
488 project.org/web/packages/nlme/index.html
489 Porada, P., Van Stan, J. T., & Kleidon, A. (2018). Significant contribution of non-vascular
490 vegetation to global rainfall interception. *Nature Geoscience, 11*, 563–567.
491 https://doi.org/10.1038/s41561-018-0176-7
492 Ray, D. K., Nair, U. S., Lawton, R. O., Welch, R. M., & Pielke Sr, R. A. (2006). Impact of land
493 use on Costa Rican tropical montane cloud forests: Sensitivity of orographic cloud
494 formation to deforestation in the plains. *Journal of Geophysical Research: Atmospheres,*
495 *111*. https://doi.org/10.1029/2005JD006096
496 Rhoades, F. M. (1995). Nonvascular epiphytes in forest canopies: worldwide distribution,
497 abundance, and ecological roles. In M. D. Lowman, & H. B. Rinker (Eds), *Forest*
498 *canopies* (pp. 353–408). San Diego, California: Academic Press.
499 Rieley, J., Richards, P., & Bebbington, A. (1979). The ecological role of bryophytes in a North
500 Wales woodland. *Journal of Ecology*, *67*, 497–527. https://doi.org/10.2307/2259109
501 Rodríguez-Quiel, E. E., Mendieta-Leiva, G., & Bader, M. Y. (2019). Elevational patterns of

bryophyte and lichen biomass differ among substrates in the tropical montane forest of Baru Volcano, Panama. *Journal of Bryology, 41*, 95–106. https://doi.org/10.1080/03736687.2019.1584433

Scholl, M., Eugster, W., & Burkard, R. (2011). Understanding the role of fog in forest hydrology: stable isotopes as tools for determining input and partitioning of cloud water in montane forests. *Hydrological Processes, 25*, 353-366. https://doi.org/10.1002/hyp.7762

Schulz, H. M., Li, C.-F., Thies, B., Chang, S.-C., & Bendix, J. (2017). Mapping the montane cloud forest of Taiwan using 12 year MODIS-derived ground fog frequency data. *PloS ONE, 12*, e0172663.

Sillett, S. C., & Antoine, M. E. (2004). Lichens and bryophytes in forest canopies. In M. D. Lowman, & H. B. Rinker (Eds), *Forest canopies* (pp. 151–174). Cambridge, Massachusetts: Academic Press. https://doi.org/10.1016/B978-012457553-0/50013-7

Smith, A. J. E. (1982). Epiphytes and epiliths. In A. J. E. Smith (Ed), *Bryophyte Ecology* (pp. 191–227). Dordrecht, Netherlands: Springer. https://doi.org/10.1007/978-94-009-5891-3_7

Stadtmüller, T. (1987). *Cloud Forests in the Humid Tropics: A Bibliographic Review*. Tokyo, Japan: United Nations University Press.

Stanton, D. E., & Reeb, C. (2016). Morphogeometric approaches to non-vascular plants. *Frontiers in Plant Science, 7*, 916. https://doi.org/10.3389/fpls.2016.00916

Still, C. J., Foster, P. N., & Schneider, S. H. (1999). Simulating the effects of climate change on tropical montane cloud forests. *Nature, 398*, 608–610. https://doi.org/10.1038/19293

Tol, G. J., & Cleef, A. M. (1994). Above-ground biomass structure of a Chusquea tessellata bamboo páramo, Chingaza National Park, Cordillera Oriental, Colombia. *Vegetatio, 115*, 29–39. https://doi.org/10.1007/BF00119384

Trynoski, S. E., & Glime, J. M. (1982). Direction and height of bryophytes on four species of northern trees. *The Bryologist*, 281–300. https://doi.org/10.2307/3243047

Turetsky, M. R. (2003). The role of bryophytes in carbon and nitrogen cycling. *The Bryologist, 106*, 395–410. https://doi.org/10.1639/05

Wang, H.-C., & Huang, C.-Y. (2012). Investigating the spatial heterogeneity of a subtropical montane cloud forest plantation with a QuickBird image. *International Journal of Remote Sensing, 33*, 7868–7885. https://doi.org/10.1080/01431161.2012.703346

Werner, F., Homeier, J., Oesker, M., & Boy, J. (2012). Epiphytic biomass of a tropical montane forest varies with topography. *Journal of Tropical Ecology, 28*, 23–31. https://doi.org/10.1017/S0266467411000526

West, G. B., Brown, J. H., & Enquist, B. J. (1997). A general model for the origin of allometric scaling laws in biology. *Science, 276*, 122–126. https://doi.org/10.1126/science.276.5309.122

West, G. B., Brown, J. H., & Enquist, B. J. (1999). A general model for the structure and allometry of plant vascular systems. *Nature, 400*, 664–667.

Ye, J., Hao, Z., & Dai, G. (2004). Bryophyte biomass in dark coniferous forest of Changbai Mountain. *The Journal of Applied Ecology, 15*, 737–740.

Zotz, G., & Bader, M. Y. (2009). Epiphytic plants in a changing world-global: change effects on vascular and non-vascular epiphytes. In U. Lüttge, W. Beyschlag, B. Büdel, & D. Francis (Eds), *Progress in Botany, vol. 70* (pp. 147–170). Berlin, Heidelberg: Springer. https://doi.org/10.1007/978-3-540-68421-3_7

Zotz, G., & Vollrath, B. (2003). The epiphyte vegetation of the palm Socratea exorrhiza-

548 correlations with tree size, tree age and bryophyte cover. *Journal of Tropical Ecology, 19*,
549 81–90. https://doi.org/10.1017/S0266467403003092

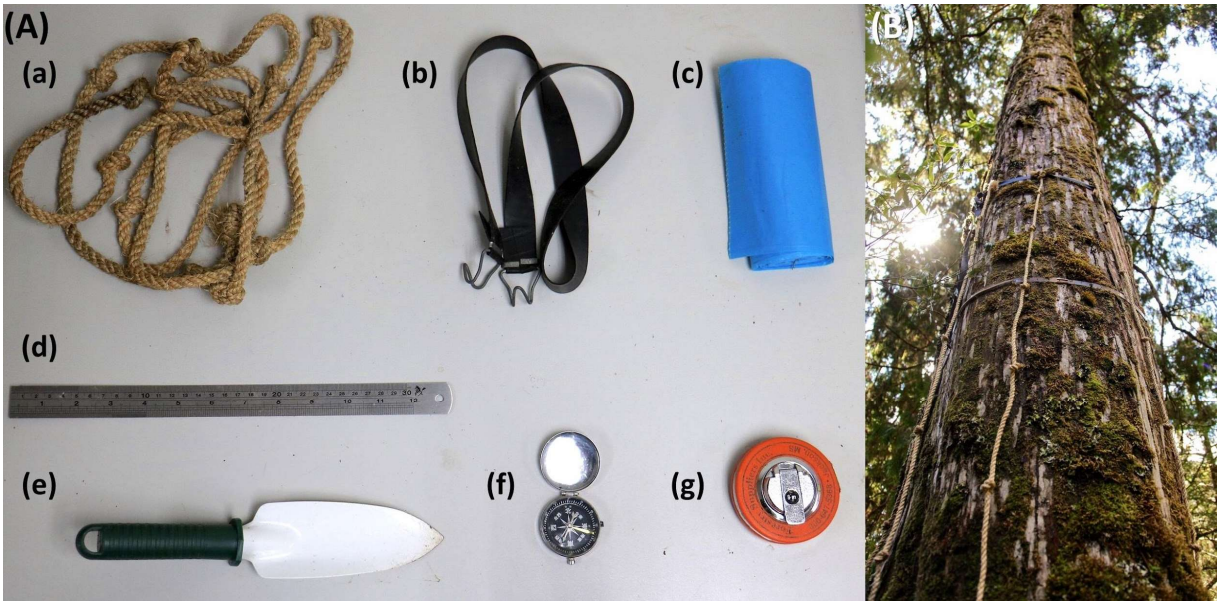

FIGURE 1 (A) The field instrument utilized in this study to estimate the biomass of epiphytic bryophytes (EB) in tropical montane cloud forests of northeastern Taiwan: (a) A 3-m rope with 30 cm long intervals marked by knots, (b) an adjustable rubber strip to fix ropes to a tree stem, (c) large, strong, and tear-resistant plastic bags to store EB from sampled stem surface area, (d) a stainless steel ruler to measure the heights of EB mats before removing samples with (e) a gardening shovel, (f) a compass to facilitate placing ropes in different orientations, (g) a fabric diameter tape to measure the sampled stem surface area. (B) A demonstration. The photograph was taken in Chilan Mountain by G. Lai in January 2019.

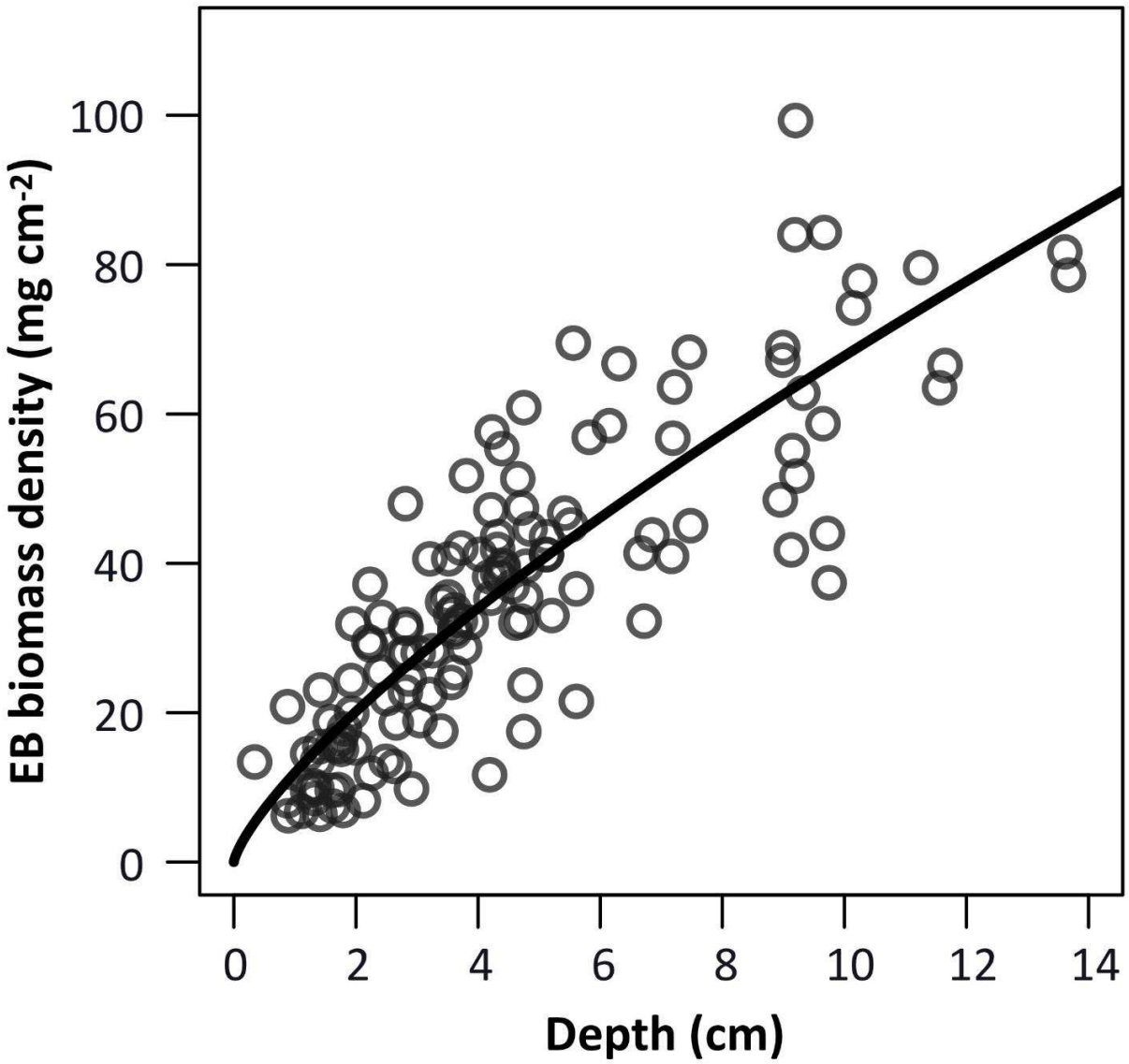

559

560 **FIGURE 2** The best empirical general depth-biomass allometric model of epiphytic bryophytes
561 (EB). The model was a power of variance covariate function ($R^2 = 0.72$, AIC = 380, $p < 0.001$, n
562 = 131), and the performance was superior to other models (Table 2) with coefficient and
563 exponent of 11.96 and 0.75, respectively.

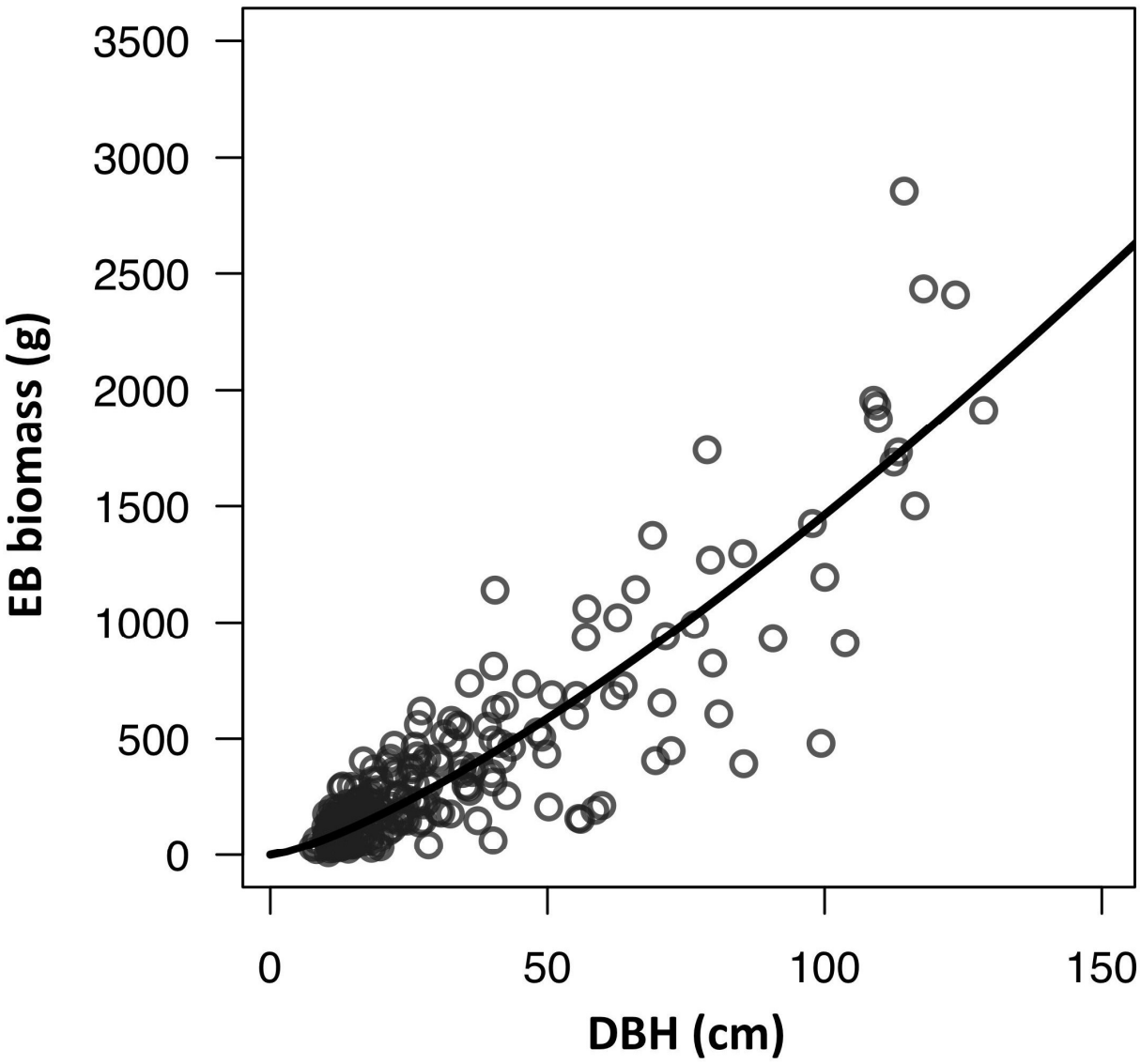

564

565 **FIGURE 3** The relationship between diameter at breast height (DBH) and epiphytic bryophyte
566 (EB) biomass of sampled stem surface area based upon 10 sampled trees of different DBH sizes
567 on the 21 field plots (n = 210, Figure S1): EB biomass = $3.40\text{DBH}^{1.32}$ ($R^2 = 0.86$, $p < 0.001$).

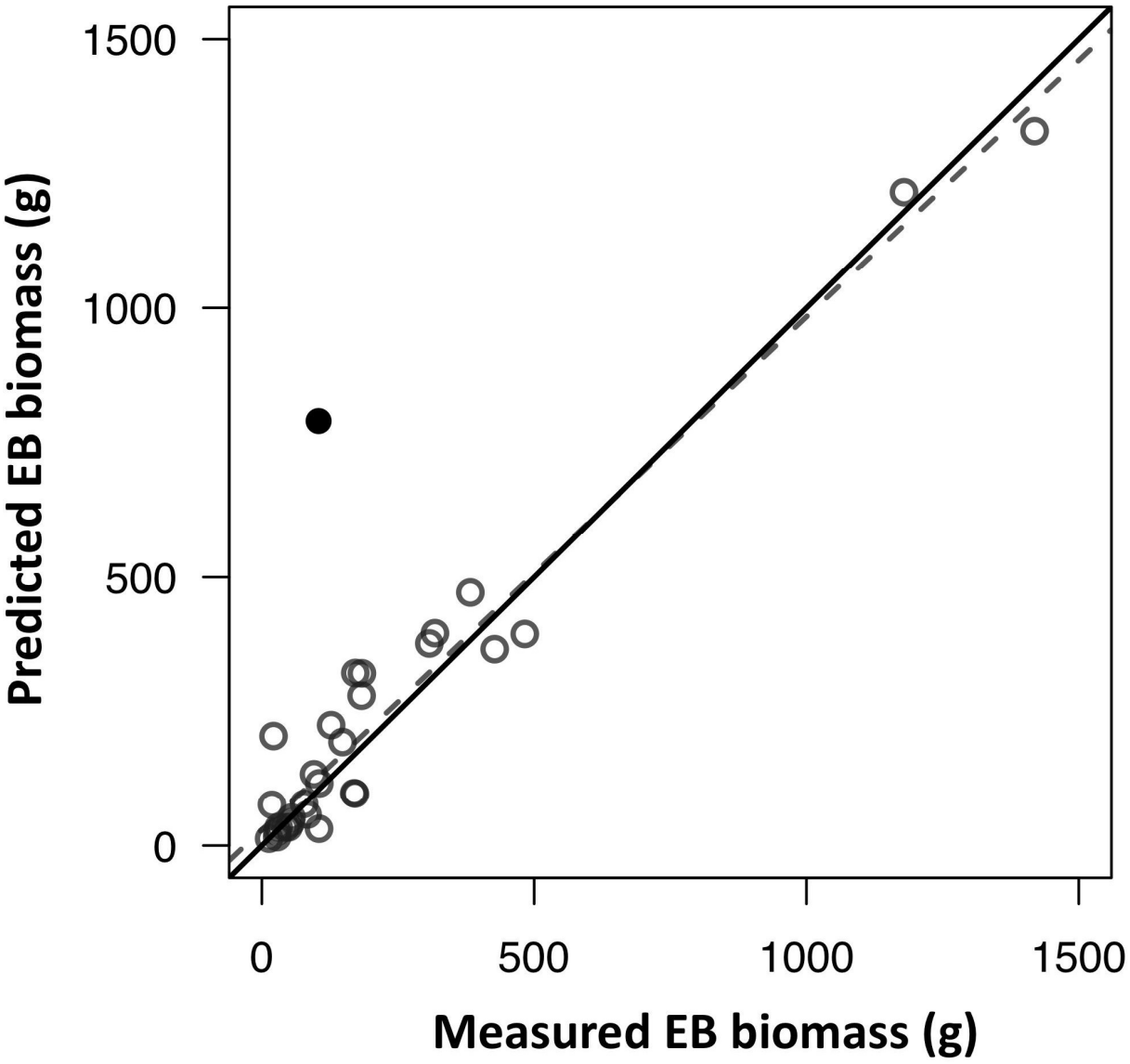

568

569 **FIGURE 4** The comparison of model-predicted epiphytic bryophyte (EB) biomass and field

570 collected EB biomass. The black solid dot indicates an apparent outlier in which EB inhabited on

571 decomposed tree bark.

572 **TABLE 1** Summary of the plot or the forest stand scale epiphytic bryophyte (EB) biomass density (kg ha^{-1}) research reported in
573 refereed literature. For the sake of quality, only peer-reviewed articles are listed. The table is organized based upon the data collection
574 methods; "Climbing" includes the use of rope or ladder, and "Ground" indicates EB samples were reachable from the ground or
575 removed from fallen logs. We note that studies that combined terrestrial bryophyte biomass or did not specify the collection of EB
576 biomass only are not listed in this table. Annual precipitation (AP, mm y^{-1}), mean annual temperature (MAT, °C) and elevation (m
577 a.s.l.) of each site were directly obtained from its corresponding article. If the information was missing, it was then obtained from the
578 internet. The ecosystems labelled as TMCF could be tropical montane cloud forest, or other similar forest ecosystems including
579 tropical montane rain forest or tropical montane moist forest. The ones categorized as TCF are temperate conifer forests. To make the
580 comparison legitimate, dead EB and humus mass was not included in the estimation. Studies only sampled part of EB biomass of trees
581 such as a tree trunk (e.g., Kürschner & Parolly, 2004) are also not listed here.

Method	Location	AP	MAT	Elevation	Ecosystem	Tree sample	EB biomass	Reference
Climbing	La Soufriére, Guadeloupe	1780	26.3	1330	TMCF	Not available	12336	Coxson (1991)
	Mascarene Archipelago, Madagascar	8000	24	1350	TMCF	Not available	9020	Ah-Peng *et al.* (2017)
	Santa Rosa de Cabal, Colombia	1250	5.5	3700	TMCF	1	6850	Hofstede, Wolf and Benzing (1993)
	Olympic Mountains, US	4700	9.6	179	TCF	3	6527	Nadkarni (1984a)
	Cordillera de Talamanca, Costa Rica	5193	16.8	1555	TMCF	15	6225	Köhler *et al.* (2007)

	Monteverde, Costa Rica	2591	18.6	1480	TMCF	25	4058	Nadkarni *et al.* (2004)
	Cordillera de Talamanca, Costa Rica	2812	10.9	2900	TMCF	6	1921	Hölscher *et al.* (2004)
	Fushan, Taiwan	3600	18.2	750	TMCF	18	1740	Hsu, Horng and Kuo (2002)
	Monteverde, Costa Rica	2591	18.6	1700	TMCF	4	945	Nadkarni (1984b)
	Northeast China	1450	-0.8	875	TCF	Not available	507	Ye, Hao and Dai (2004)
	The Tilaran Range, Costa Rica	5380	17.7	1325	TMCF	6	206	Häger and Dohrenbusch (2011)
Harvesting	Monteverde, Costa Rica	2591	18.6	1480	TMCF	9	2087	Nadkarni *et al.* (2004)
	Yunnan, China	1931	11.3	2500	TMCF	77	1663	Chen, Liu and Wang (2010)
	Cordillera Oriental, Colombia	1850	6	3650	Bamboo	Not available	1281	Tol and Cleef (1994)
	Rwenzor Mountains, Uganda	2000	8.5	3230	TMCF	1	1000	Pentecost (1998)
	Marafunga Basin, New Guinea	3985	13	2625	TMCF	42	940	Edwards and Grubb (1977)
	Zamora Chinchipe, Ecuador	2080	15.5	2093	TMCF	63	604	Werner *et al.* (2012)

		Central French Guiana	2500	27	288	TMCF	15	452	Gehrig-Downie *et al.* (2011)
		Cascade Range, US	2450	9.2	655	TCF	42	323	McCune (1993)
	Ground	Southern Thailand	2000	28.5	804	Tropical forests	51	126	Chantanaorrapint and Frahm (2011)
		North Wales, UK	2187	10.3	98	TCF	16	87	Rieley, Richards and Bebbington (1979)
	Scaling	Chilan mountain, Taiwan	3500	12.7	1680	TMCF	210	272	This study

582

583 **TABLE 2** Model performance comparison of allometric equations ($W = \alpha D^{\beta}$, equation (1)) by referring to values of the Akaike
584 Information Criterion (AIC), the Bayesian Information Criterion (BIC) and log likelihood. We note that all models are significant with
585 $p < 0.001$.

Model	α	β	R^2	AIC	BIC	Log likelihood
Nonlinear squared regression	12.62	0.72	0.72	395.12	403.75	-194.56
Nonlinear squared regression*	10.00	0.84	0.70	400.34	406.09	-198.17
Power of a variance covariate	11.96	0.75	0.72	379.92	391.43	-185.96
Exponential of a variance covariate	11.77	0.77	0.72	380.12	391.62	-186.06
Constant power of a variance covariate	11.78	0.76	0.70	380.91	395.28	-185.45

586 *Nonlinear squared regression with the fixed α of 10.00